Acta Biochim Biophys Sin 2024, 56(11): 1644–1658
https://doi.org/10.3724/abbs.2024102
Advance Access Publication Date: 8 July 2024
Original Article

Original Article

Acetyl-11-keto-β-boswellic acid restrains the progression of synovitis in osteoarthritis via the Nrf2/HO-1 pathway

Jing Zhou[1,2,†], Xueyan Li[2,3,†], Zeyu Han[4,†], Yinhua Qian[1,2], Lang Bai[1,2], Qibin Han[1,2], Maofeng Gao[5], Yi Xue[6], Dechun Geng[5,*], Xing Yang[1,2,*], and Yuefeng Hao[1,2,*]

[1]Orthopedics and Sports Medicine Center, the Affiliated Suzhou Hospital of Nanjing Medical University, Suzhou 215006, China, [2]Gusu School, Nanjing Medical University, Suzhou 215006, China, [3]Department of Anesthesia, the Affiliated Suzhou Hospital of Nanjing Medical University, Suzhou 215006, China, [4]Department of Foot and Ankle Surgery, Beijing Tongren Hospital, Capital Medical University, Beijing 100730, China, [5]Department of Orthopaedics, the First Affiliated Hospital of Soochow University, Suzhou 215006, China, and [6]Department of Orthopaedics, Changshu Hospital Affiliated to Nanjing University of Traditional Chinese Medicine, Suzhou 215500, China
[†]These authors contributed equally to this work.
*Correspondence address. Tel: +86-13913109339; E-mail: haoyuefeng@njmu.edu.cn (Y.H.) / Tel: +86-15962122138; E-mail: xingyangsz@126.com (X.Y.) / Tel: +86-13915439672; E-mail: szgengdc@163.com (D.G.)

Received 15 January 2024 Accepted 1 April 2024

Abstract
Synovial inflammation plays a key role in osteoarthritis (OA) pathogenesis. Fibroblast-like synoviocytes (FLSs) represent a distinct cell subpopulation within the synovium, and their unique phenotypic alterations are considered significant contributors to inflammation and fibrotic responses. The underlying mechanism by which acetyl-11-keto-β-boswellic acid (AKBA) modulates FLS activation remains unclear. This study aims to assess the beneficial effects of AKBA through both *in vitro* and *in vivo* investigations. Network pharmacology evaluation is used to identify potential targets of AKBA in OA. We evaluate the effects of AKBA on FLSs activation *in vitro* and the regulatory role of AKBA on the Nrf2/HO-1 signaling pathway. ML385 (an Nrf2 inhibitor) is used to verify the binding of AKBA to its target in FLSs. We validate the *in vivo* efficacy of AKBA in alleviating OA using anterior cruciate ligament transection and destabilization of the medial meniscus (ACLT+DMM) in a rat model. Network pharmacological analysis reveals the potential effect of AKBA on OA. AKBA effectively attenuates lipopolysaccharide (LPS)-induced abnormal migration and invasion and the production of inflammatory mediators, matrix metalloproteinases (MMPs), and reactive oxygen species (ROS) in FLSs, contributing to the restoration of the synovial microenvironment. After treatment with ML385, the effect of AKBA on FLSs is reversed. *In vivo* studies demonstrate that AKBA mitigates synovial inflammation and fibrotic responses induced by ACLT+DMM in rats via activation of the Nrf2/HO-1 axis. AKBA exhibits theoretical potential for alleviating OA progression through the Nrf2/HO-1 pathway and represents a viable therapeutic candidate for this patient population.

Key words osteoarthritis, fibroblast-like synoviocytes, acetyl-11-keto-β-boswellic acid, Nrf2, oxidative stress, reactive oxygen species

Introduction

Osteoarthritis (OA) is a prevalent musculoskeletal disorder characterized by substantial morbidity and disability [1]. The management of OA has become a significant public health concern worldwide. Nevertheless, while treatments for OA primarily focus on providing symptomatic relief and do not effectively halt or reverse disease progression, they may result in long-term side effects, such as joint infections [2]. Despite extensive research efforts over the years, the pathogenesis of OA remains poorly understood, and the availability of effective treatments is limited. Consequently, it is crucial to further elucidate the underlying mechanisms of OA to find novel approaches for early prevention and treatment. OA is a degenerative joint disease that impacts various components of the joint, including cartilage, subchondral bone, and synovium [3–5]. Synovial inflammation is recognized as a significant pathological characteristic in the early stage of OA and

is closely associated with clinical symptoms [6,7]. Recent research has highlighted the crucial role of fibroblast-like synoviocytes (FLSs), which are mesenchymal cells that reside in synovial tissue, in the aberrant activation and biological function alterations observed during the progression of OA [8]. Research on the molecular mechanisms underlying these abnormalities holds practical significance for pinpointing precise targets and developing novel drugs for the prevention and treatment of OA.

Oxidative stress arises from the dysregulation of reactive oxygen species (ROS) and reactive nitrogen species (RNS) produced during metabolic activities in the body, as well as the concomitant antioxidant defense system, resulting in elevated levels of oxidants [9,10]. Under physiological conditions, ROS and RNS engage in various metabolic pathways to safeguard cells from oxidative damage. The nuclear factor erythroid 2-related factor 2 (Nrf2) serves as the principal orchestrator of the organism's reaction to oxidative stress, exerting a pivotal influence on cellular processes and inflammation by regulating oxidative stress [11,12]. Upon encountering external stimuli, the Nrf2/kelch-like ECH-associated protein 1 (Keap1) complex disassembles, liberating Nrf2 into the nucleus and instigating subsequent gene transcription. In individuals with OA, inflammatory reactions and alterations in the local microenvironment within the joints can prompt synovial hypoxia, consequently promoting heightened metabolic activity in FLSs [13–15]. This heightened activity leads to the secretion of inflammatory mediators [16], ROS [17], and matrix metalloproteinases (MMPs) [18], culminating in oxidative damage and an inflammatory cascade. Hence, ROS-induced oxidative stress may play a role in the initiation of synovial inflammation and contribute significantly to the distinctive phenotype exhibited by OA-FLSs [19–21]. Nevertheless, the exact mechanism by which increased ROS levels regulate specific phenotypic alterations in OA-FLSs and the inflammatory milieu within the synovium remains a pertinent unresolved question.

Recent studies have demonstrated that specific low-toxicity small molecule compounds sourced from traditional Chinese medicine, including agnuside [22], gallic acid [23], and naringenin [24], inhibit synovitis in OA by attenuating ROS, inflammation and MMPs. Additionally, frankincense resin, a historically esteemed traditional medicinal remedy in India and China, has exhibited potential for mitigating OA symptoms [25]. Acetyl-11-keto-β-boswellic acid (AKBA), identified as the most potent compound found in frankincense, exhibits considerable promise in various domains, as evidenced by a multitude of studies highlighting its anti-inflammatory [26], analgesic[27], antioxidant [28], antitumorigenic [29], immunomodulatory [30], and lipid-regulatory [31] properties. Numerous studies have established a correlation between AKBA and synovial lesions, with some indicating its potential efficacy in alleviating symptoms of OA. Considering the considerable influence of ROS on FLSs and the potential inhibitory effects of AKBA on ROS, we postulated that AKBA may regulate phenotypic alterations in FLSs by reducing ROS levels, thereby influencing the progression of OA.

This study examined the impact of AKBA intervention on surgery, lipopolysaccharide (LPS)-induced inflammation, MMPs, and ROS. The results suggest that AKBA intervention significantly decreases the secretion of inflammatory cytokines, MMPs, and ROS. This decrease in inflammation, MMPs, and ROS was facilitated by the activation of the Nrf2/HO-1 signaling pathway by AKBA. In summary, our findings offer dedicated support for the use of AKBA as a viable therapeutic approach for the management and mitigation of OA.

Materials and Methods

Retrieval of AKBA and OA targets and protein-protein interaction (PPI) network construction

We used the Swiss Target Prediction (http://www.swisstargetprediction.ch/) and SuperPred (https://prediction.charite.de/index.php) databases to identify all the targets linked to AKBA. The identified targets were then cross-referenced with data from UniProt (https://www.uniprot.org/) to guarantee precision. Non-human genes were eliminated, duplicate targets were removed, and gene nomenclature was standardized. To compile targets related to OA, keyword searches were conducted in the GeneCards (https://www.genecards.org/), Online Mendelian Inheritance in Man (OMIM: https://www.omim.org/), and Therapeutic Target Database (TTD, https://www.ttd.org/) databases. Targets sourced from three databases were consolidated into an Excel spreadsheet, and duplicate genes were eliminated. Validation of disease target gene data was conducted utilizing the UniProt database. Subsequently, the targets of the drug component (AKBA) and the disease (OA) were cross-referenced to identify common genes. A Venn diagram was created to illustrate the overlap of these genes. The "drug-target" network was constructed using Cytoscape 3.7.2 software.

In order to investigate the protein-protein interactions influenced by AKBA during OA treatment, we utilized the Search Tool for the Retrieval of Interacting Genes/Proteins (STRING) database (https://string-db.org/) to generate a protein-protein interaction (PPI) network based on the intersecting gene list. The analysis was restricted to the species "Homosapiens", with a minimum interaction score of 0.7 implemented to ensure the reliability of the study. Default parameters were maintained, and the results were exported in TSV format for further analysis in Cytoscape 3.7.2. Network analysis was carried out using the Cytoscape Tools Network Analyzer, and the results were saved for subsequent investigation.

Gene Ontology (GO) and Kyoto Encyclopedia of Genes and Genomes (KEGG) signaling pathway enrichment analysis of co-targets

The genes associated with both AKBA and OA were input into the Database for Annotation, Visualization and Integrated Discovery (DAVID, https://david.ncifcrf.gov/summary.jsp), utilizing OFFICIAL_GENE_SYMBOL as the gene identifier and specifying the species as *Homo sapiens*. DAVID 6.8 GO gene function analysis was employed to examine the roles of AKBA in OA treatment, focusing on biological process (BP), cellular component (CC), and molecular function (MF) terms. To clarify the treatment targets of AKBA for OA, a KEGG pathway enrichment analysis was performed. The top 10 items related to OA in GO functions (BP, CC, and MF) and the top 20 pathways (with a significance level of $P<0.05$) in the KEGG pathways were selected. These processes and signaling pathways are the principal functional enrichment pathways and mechanisms of action of AKBA in treating OA.

Chemicals

AKBA (purity of 99.93%, HY-N0892, MedChemExpress, Monmouth Junction, USA), LPS (HY-D1056, MedChemExpress, experimental concentration: 1 μg/mL), and ML385 (purity of 99.96%, HY-100523, MedChemExpress, concentration: 10 μM) were utilized for *in vitro* and *in vivo* experiments. DMSO was used as the solvent for

preparing the stock solutions, which were stored at −80°C.

Cell culture

Rat primary FLSs (Cat No. CP-R329; Procell Life Technology, Wuhan, China) were cultured in F12 medium (Gibco, Waltham, USA) supplemented with 10% fetal bovine serum (FBS; Procell) and 1% penicillin/streptomycin (PS; NCM, Suzhou, China) following digestion with 0.25% trypsin (NCM). The cells were maintained in a standard incubator at 37°C with 5% CO_2, and the medium was changed every 3 days. Subculturing was carried out when the cells reached 70%–80% confluency after appropriate washing and digestion procedures. Non-FLSs were present in primary cells after three generations of culture, and to ensure the stability of the cell phenotype, we selected $P_{4\text{-}6}$ FLSs for *in vitro* experiments.

Cell viability assay

FLSs were cultured in 96-well plates at a seeding density of 5×10^3 cells per well in 100 μL of F12 medium. Subsequently, the FLSs were exposed to varying concentrations of AKBA (0, 2, 4, 8, 16, or 32 μM) for 24, 48, or 72 h post-adherence. At specified time intervals, the cells were rinsed with phosphate-buffered saline (PBS) and incubated with cell counting kit-8 (CCK-8) reagent (Dojindo, Shanghai, China) for 3 h at 37°C. The optical density (OD) was recorded at 450 nm to assess cell viability. The cell viability relative to that of the control group was calculated using the following equation: cell viability to control (%)=OD of drug-treated group/OD of control group.

Cell migration and invasion assays and cell scratching assay

Cell migration and invasion assays were performed using transwell inserts (Corning, New York, USA). A total of 2×10^5 cells were suspended in 200 μL of F12 medium without FBS and seeded into cell culture plates that were either precoated with 1 μg/mL Matrigel (Corning) (invasion) or left uncoated (migration). Transfected cells (5×10^4/well) were seeded in culture medium supplemented with 1% FBS and added to the upper chamber of the transwell filter. The cells were incubated at 37°C in 95% air for half a day and then fixed in 4% paraformaldehyde. The staining process was achieved with 0.1% crystal violet (Sigma-Aldrich, Shanghai, China). The degree of cell migration and invasion was observed using an AxioCam HRc microscope (Carl Zeiss, Wetzlar, Germany).

After treatment with 10 mg/mL mitomycin C (Sigma-Aldrich) for 2 h, a confluent monolayer was formed within 24 h by cells cultured in a six-well plate. The monolayer was then scratched with a sterile pipette tip, FLSs were treated with or without LPS or AKBA, the cells were washed with PBS two times, and the wound areas were photographed before and after incubation.

Western blot analysis

Protein extraction from FLSs was carried out using RIPA lysis buffer supplemented with 1 mM phenylmethanesulfonyl fluoride (PMSF), followed by centrifugation at 16,000 *g* for 12 min at 4°C. The protein concentration was quantified using a BCA protein assay kit (NCM). The extracted proteins were then separated on SDS-polyacrylamide gels with varying concentrations of 7.5%, 10%, or 12.5% (w/v) and subsequently transferred onto polyvinylidene fluoride (PVDF) membranes (Bio-Rad, Hercules, USA). The membranes were blocked with a 5% (w/v) milk solution for 1 h at room temperature, followed by overnight incubation at 4°C with primary antibodies targeting IL-1β (AF5103, 1:1000; Affinity, Changzhou, China), IL-6 (DF6087, 1:1000; Affinity), TNF-α (AF7014, 1:500; Affinity), iNOS (18985-1-AP, 1:1000; Proteintech, Rosemont, USA), COX-2 (66351-1-Ig, 1:1000; Proteintech), MMP-1 (10371-2-AP, 1:1000; Proteintech), MMP-3 (17873-1-AP, 1:1000; Proteintech), MMP-13 (18165-1-AP, 1:1000;), Nrf2 (16396-1-AP, 1:2000; Proteintech), Keap1 (10503-2-AP, 1:2000; Proteintech), HO-1 (10701-1-AP, 1:1000; Proteintech), NQO1 (67240-1-Ig, 1:5000; Proteintech), β-actin (20536-1-AP, 1:5000; Proteintech), and Histone H3 (68345-1-Ig, 1:10000; Proteintech). Subsequently, the membranes were rinsed three times with TBS supplemented with 0.05% Tween 20 (TBST) and then incubated with horseradish peroxidase-conjugated secondary antibodies (goat anti rabbit-A0208 & goat anti mouse-A0216 1:1000; Beyotime, Shanghai, China) for 1 h. The resulting signals were observed utilizing a ChemiDocXRS+Imaging System (Tanon, Shanghai, China). Each experiment was repeated three times.

Quantitative real-time PCR

Total RNA was isolated using TRIzol (Beyotime) and quantified by spectrophotometry. Subsequently, RNA from each experimental group was reverse transcribed utilizing the Prime Script RT reagent Kit (Beyotime). Primers were designed and synthesized by Shanghai Biotechnology Service Company (Shanghai, China), following the gene sequence in GenBank designed with Oligo v6.6 software (sequences listed in Table 1). The qPCR analysis was performed using a LightCycler 480 II instrument (Roche, Basel, Switzerland) and a Premix Ex Taq SYBR-Green PCR kit (Takara, Kyoto, Japan) following the manufacturer's instructions. The mRNA

Table 1. Sequences of primers used in PCR

Gene	Primer sequence Forward (5′→3′)	Reverse (3′→5′)
IL-1β	CAGCTATGGCAACTGTCCCT	AACAGGTCATTCTCCTCACTGT
IL-6	GCCCACCAGGAACGAAAGTC	ACTGGCTGGAAGTCTCTTGCG
TNF-α	GAGGCAACACATCTCCCTCC	TCCGCTTGGTGGTTTGCTAC
iNOS	GCCTAGTCAACTACAAGCCCCA	TTGATCCTCACGTGCTGTGG
COX-2	ATCCTTGCTGTTCCAACCCA	TCTTGTCAGAAACTCAGGCGTA
MMP-1	CATCCAGGCTTTATATGGGCCTT	GCGTCGAAGGTTAGATCACCA
MMP-3	GCTGTCTTTGAAGCATTTGGGTT	CCTCCATGAAAAGACTCAGAGGAA
MMP-13	TCTTGAGTTTGCAGAGCACTACT	CCACATCAGGCACTCCACAT
GAPDH	ACTGGCGTCTTCACCACCAT	AAGGCCATGCCAGTGAGCTT

expression levels of individual genes were normalized to that of the *GAPDH* reference gene and determined using the $2^{-\Delta\Delta Ct}$ method.

Immunofluorescence staining

The cells were subjected to a sequential protocol involving washing with PBS, fixing in 4% paraformaldehyde, and permeabilizing with 0.1% Triton X-100 for 15 min. Subsequent steps included blocking with 5% bovine serum albumin at 37°C for 1 h, followed by overnight incubation with primary antibodies specific for Nrf2 (16396-1-AP, 1:200; Proteintech) overnight at 4°C. Following wash with PBS, the cells were incubated for 1 h at 37°C with FITC-conjugated secondary antibodies (AS011, 1:200; ABclonal, Wuhan, China) and TRITC-conjugated phalloidin (40734ES75, 1:200; Yeasen, Shanghai, China), followed by 7 min of staining with DAPI (Beyotime). For observation, 10 fields from each slide were randomly selected and examined using a fluorescence microscope (Carl Zeiss).

Animal study

The animal experiments conducted in this study were ethically approved by the Ethics Committee of the Affiliated Suzhou Hospital of Nanjing Medical University. Thirty male Sprague-Dawley (SD) rats, aged 6 weeks and weighing 200–250 g, were procured from the Animal Core Facility of Nanjing Medical University. The rats were housed in a controlled environment with access to adequate water and food. An anterior cruciate ligament transection and destabilization of the medial meniscus (ACLT+DMM) OA model was successfully established in these rats. The SD rats were randomly allocated into three groups: Sham, OA, and OA+AKBA (n=10 rats per group). Anesthesia was induced using isoflurane for all rats. Subsequently, the surgical site on the right hind limb was shaved and disinfected in accordance with aseptic procedures. A longitudinal skin incision was then made to expose the knee joint, followed by excision of the medial collateral ligament. The medial meniscus and anterior cruciate ligament were surgically excised while preserving the integrity of the articular cartilage surface. The joint cavity and skin were meticulously sutured using 3-0 silk thread in a layered fashion. Notably, postoperative immobilization of the affected limb was not implemented, and the experimental animals were returned to their housing facility for continued care. Following a two-week period of modeling, the rats were treated with intraperitoneal injections of either 0.5 mL/kg saline or 8 mg/kg AKBA solution on alternate days for 4 weeks. Subsequently, all experimental animals were euthanized after 8 weeks, and samples were collected for subsequent analyses.

Pain sensitivity test, body weight, and knee joint diameter measurement

The differences in nociceptive responses to mechanical stimuli in rats were examined through the use of an electronic von Frey system (Dynamic Plantar Aesthesiometer, Ugo Basile, Italy). Before each trial, the rats were acclimated for 30 min within transparent Perspex chambers placed on a metal mesh floor, allowing precise targeting of the stimulation needle tip to the midplantar region of the limb under study. Each test was repeated at least 3 times, with a minimum interval of 10 min between consecutive stimuli. Statistical analysis was conducted by averaging the results of 3 tests. Rats were weighed biweekly using an electronic balance after a 12-h fasting period. The joint diameter of the right hind limb was measured in the relative horizontal position using a Vernier caliper.

Histopathologic analysis

Samples from each group were subjected to decalcification by immersion in 10% ethylenediaminetetraacetic acid (EDTA) for 4 weeks. Following decalcification, the paraffin-embedded samples were sectioned into 6-μm slices and stained with hematoxylin and eosin (H&E), Sirius red, safranin O-fast green (SO-FG), and toluidine blue (TB) according to the manufacturer's recommended protocols [32]. In brief, the slices were soaked in different corresponding dyes, washed with water, and sealed with xylene transparent and neutral gum. Image capture was performed using an AxioCam HRc microscope (Carl Zeiss).

Immunohistochemical staining

For immunohistochemistry analysis, thin paraffin-embedded tissue sections (6 μm) were treated with 3% (v/v) hydrogen peroxide for 10 min, followed by three times wash with PBS and incubation with pepsin at 37°C for 30 min. Subsequently, the tissue sections were blocked with 10% (v/v) goat serum albumin for 30 min at 37°C. The sections were incubated overnight at 4°C with specific primary antibodies targeting Nrf2 (16396-1-AP, 1:200; Proteintech), HO-1 (10701-1-AP, 1:200; Proteintech), iNOS (18985-1-AP, 1:200; Proteintech), Col II (28459-1-AP, 1:200; Proteintech), and MMP-13 (18165-1-AP, 1:200; Proteintech). In the Sham group, tissue sections were incubated with nonspecific IgG, followed by incubation with secondary antibodies conjugated with HRP and subsequent staining with hematoxylin.

Statistical analysis

Data were presented as the mean±standard deviation (SD). All experiments were conducted in triplicate. Data analysis was carried out using GraphPad Prism 9 (Graphpad software, La Jolla, USA), with comparisons between two groups made using an unpaired two-tailed Student's t-test. Multiple group comparisons were performed using one-way analysis of variance (ANOVA) followed by a Bonferroni post-hoc test. Statistical significance was established at a threshold of P<0.05.

Results

Bioinformatics analysis of AKBA and OA

We utilized Swiss Target Prediction to identify 98 potential targets of AKBA with a probability>0. Subsequently, 101 targets were identified using SuperPred. After eliminating duplicates, we obtained a total of 184 targets corresponding to all components of AKBA. The GeneCards and OMIM databases were utilized to identify 5030 and 33 targets associated with OA, respectively. After cross-referencing with the UniProt database and removing redundancies, 5069 targets linked to weight gain in OA were identified. The cross-referencing of AKBA and OA targets revealed 107 OA-drug cross-correlated target genes that could serve as potential interaction targets for OA drug therapy (Figure 1A). Prominent targets include NOS2, PTGS2, MMP1, and MMP3, which are implicated in inflammation and MMPs (Figure 1B).

A GO enrichment analysis was performed, revealing 345 GO terms that met a significance threshold of P<0.05, to elucidate the role of AKBA in OA. Among these genes, 220 were related to biological processes (BP), with a focus on the regulation of the inflammatory response and reactive oxygen species metabolic processes. Additionally, 58 entries related to cellular components (CC), specifically involving the plasma membrane, cytoplasm,

nucleoplasm, and extracellular regions, were identified. Among these genes, 66 were found to be associated with molecular function (MF), notably nuclear receptor activity (Figure 1C). Through the utilization of the DAVID database, pathway enrichment analysis revealed a total of 109 pathways enriched in the role of AKBA in OA. Notably, 95 of these pathways were found to have a significance level of $P<0.05$, with the Nrf2 signaling pathway ranking among the top 20 (Figure 1D).

AKBA reduces LPS-induced migration and the expression of inflammatory cytokines and MMPs in FLSs

The chemical structure of AKBA is presented in Figure 2A. The cytotoxicity of AKBA was assessed at various concentrations (0, 1, 2, 4, 8, 16, and 32 μM) in rat FLSs after 24, 48, and 72 h (Figure 2B, C). After 72 h of treatment with 16 μM AKBA, a notable decrease in cell viability was observed ($P<0.05$), suggesting that AKBA concentrations between 1 and 8 μM did not induce significant cytotoxic effects. Consequently, an AKBA concentration of 8 μM was chosen for subsequent experiments.

To further investigate the effects of AKBA on FLS properties, migration and invasion assays were performed on AKBA-treated FLSs using a transwell chamber and a cell scratch assay. Treatment with 8 μM AKBA resulted in a significant decrease in the migratory and invasive capabilities of FLSs compared to those in the control group (Figure 2D,E). It is widely recognized that inflammatory cytokines and MMPs are key factors in the migration and invasion of OA-FLSs. To clarify the influence of AKBA on the regulation of these factors, the protein and mRNA levels of IL-1β, IL-6, TNF-α, iNOS, COX-2, MMP-1, MMP-3, and MMP-13 were quantified in FLSs following stimulation with LPS and subsequent treatment with 8 μM AKBA for 24 h. The results indicated that LPS induced an increase in the protein expressions of inflammatory cytokines and MMPs, a response that was mitigated by AKBA intervention (Figure 2F). Furthermore, parallel studies were conducted to evaluate the impact of AKBA on mRNA expression induced by LPS. The observed trends in mRNA levels aligned with the patterns observed at the protein level (Figure 2G). In conclusion, these findings indicate that AKBA may play a role in diminishing inflammatory cytokines and MMPs in OA-FLSs.

AKBA reduces ROS levels and increases the nuclear translocation of Nrf2 in FLSs.

Oxidative stress, arising from an imbalance between ROS generated by the body's metabolic processes and antioxidant defense

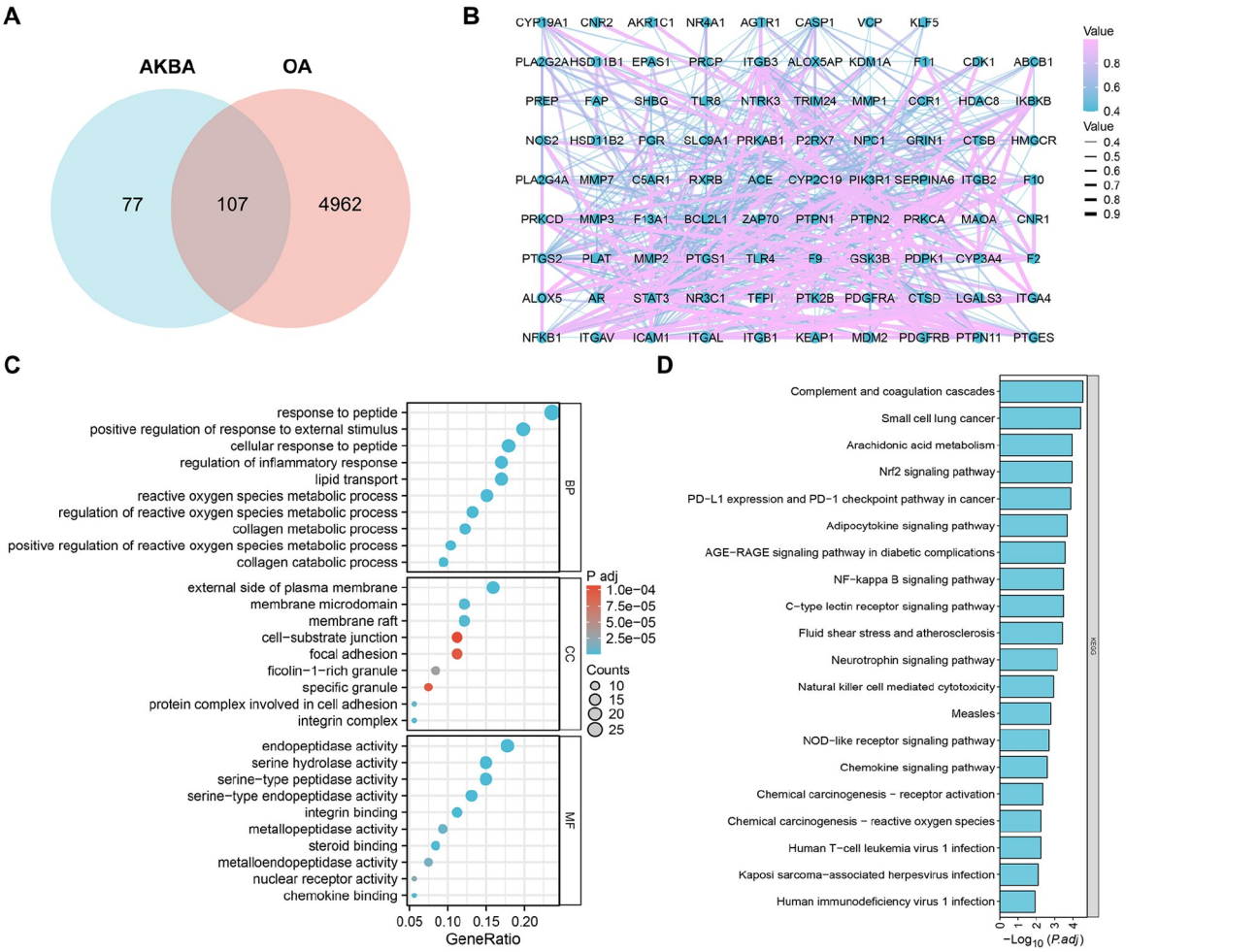

Figure 1. Network pharmacological analysis (A) Common targets of AKBA and OA. (B) Network relationship of co-targets between AKBA and OA. (C) The top 10 items from the GO analysis for biological process (BP), cellular component (CC), and molecular function (MF). (D) The top 20 pathways of co-targets.

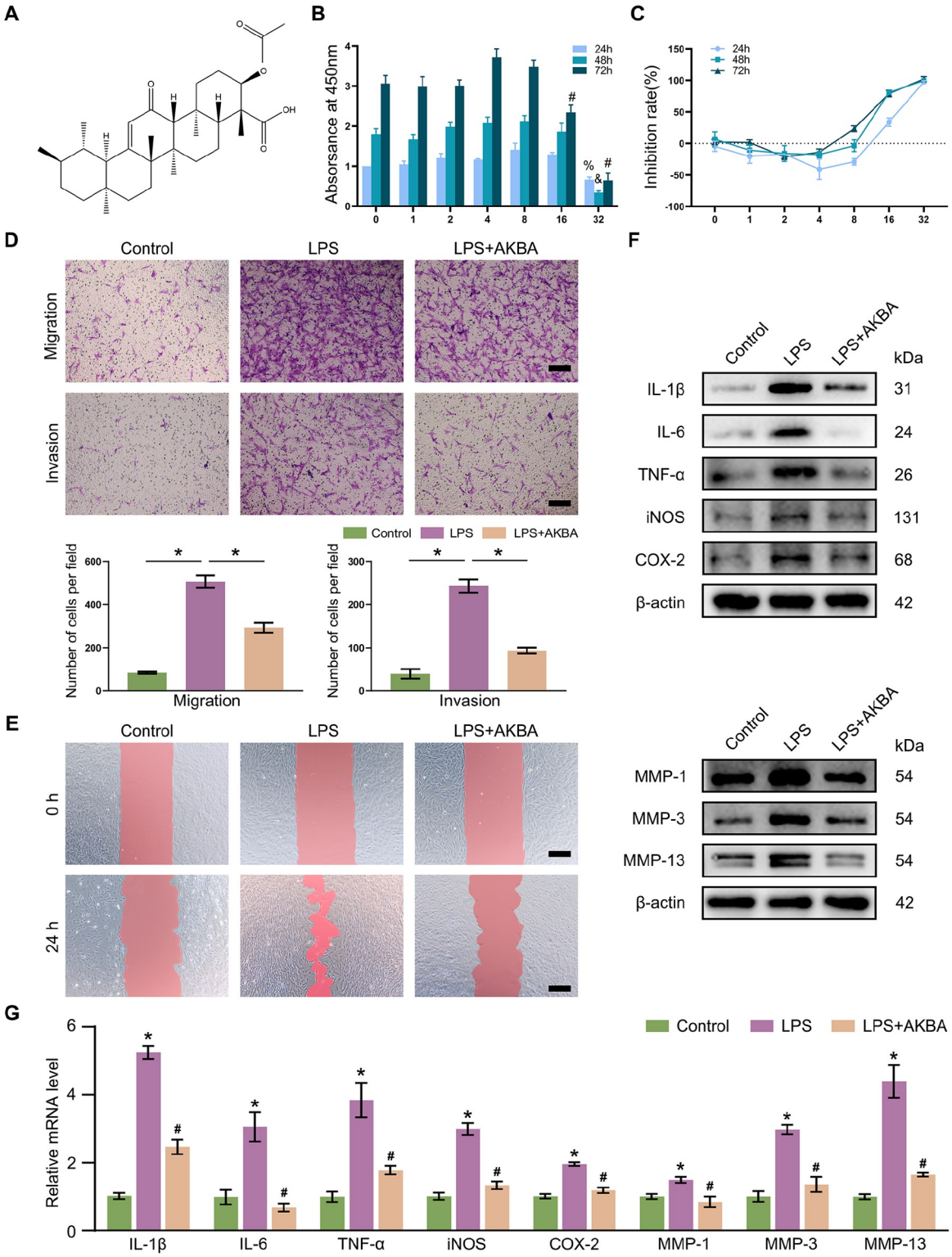

Figure 2. AKBA reduces LPS-induced migration and the expression of inflammatory cytokines and MMPs in FLSs (A) Chemical structure of AKBA. (B, C) The cytotoxic effect of AKBA (0, 1, 2, 4, 8, 16, 32 μM) on FLSs was determined at 24, 48, and 72 h by CCK-8 assays; $^{\%}P<0.05$ (24 h), $^{\&}P<0.05$ (48 h), and $^{\#}P<0.05$ (72 h) vs. the 0 μM group. (D) Transwell migration and invasion assays and quantitative analysis of FLSs; scale bar: 200 μm. $^{*}P<0.05$ vs. the control group. (E) Wound healing detected by cell scratch assay; scale bar: 200 μm. (F) Representative western blot analysis of inflammatory cytokines and MMPs protein expressions in AKBA-treated FLSs. (G) qPCR analysis of inflammatory cytokines and MMPs mRNA expression in AKBA-treated FLSs; $^{*}P<0.05$ vs the control group, $^{\#}P<0.05$ vs the LPS group. Data are expressed as the mean±SD, $n=3$.

mechanisms, has been implicated in the pathogenesis of OA [33]. To investigate the underlying mechanism of the antioxidative stress effect of AKBA, we initially examined ROS levels in LPS-treated FLSs treated with or without AKBA. The redox status of FLSs was assessed by measuring ROS levels using immunofluorescence and flow cytometry with 2′, 7′-Dichlorofluorescin diacetate (H2DCFDA) dye. As shown in Figure 3A–D, LPS-stimulated FLSs exhibited increased ROS levels, which were decreased following AKBA treatment.

Nrf2 is synthesized and accumulates in the cytoplasm before translocating to the nucleus to activate the expressions of its target phase II genes, such as heme oxygenase-1 (*HO-1*) and quinone oxidoreductase 1 (*NQO1*). Keap1 forms a complex with Nrf2, serving as the primary negative regulator of Nrf2 activity [34]. Consequently, nuclear and cytoplasmic proteins were isolated and analyzed for Nrf2 and Keap1 expression using western blot analysis. The findings indicated a significant upregulation of Nrf2 expression in the nucleus upon LPS stimulation, which was further augmented by AKBA treatment, while no notable alteration was observed in the cytoplasm (Figure 3E,F). Moreover, there was no significant difference in the expression of Keap1 in either the nucleus or cytoplasm of FLSs (Figure 3E,F). Furthermore, the upregulation of downstream proteins of Nrf2, specifically HO-1 and NQO1, was observed in FLSs following treatment with AKBA (Figure 3G). Immunofluorescence staining of FLSs revealed a greater nuclear density of Nrf2 in the LPS+AKBA group than in the LPS and control groups (Figure 3H). These results collectively suggest that AKBA functions to mitigate oxidative stress by enhancing Nrf2 expression and facilitating its nuclear translocation.

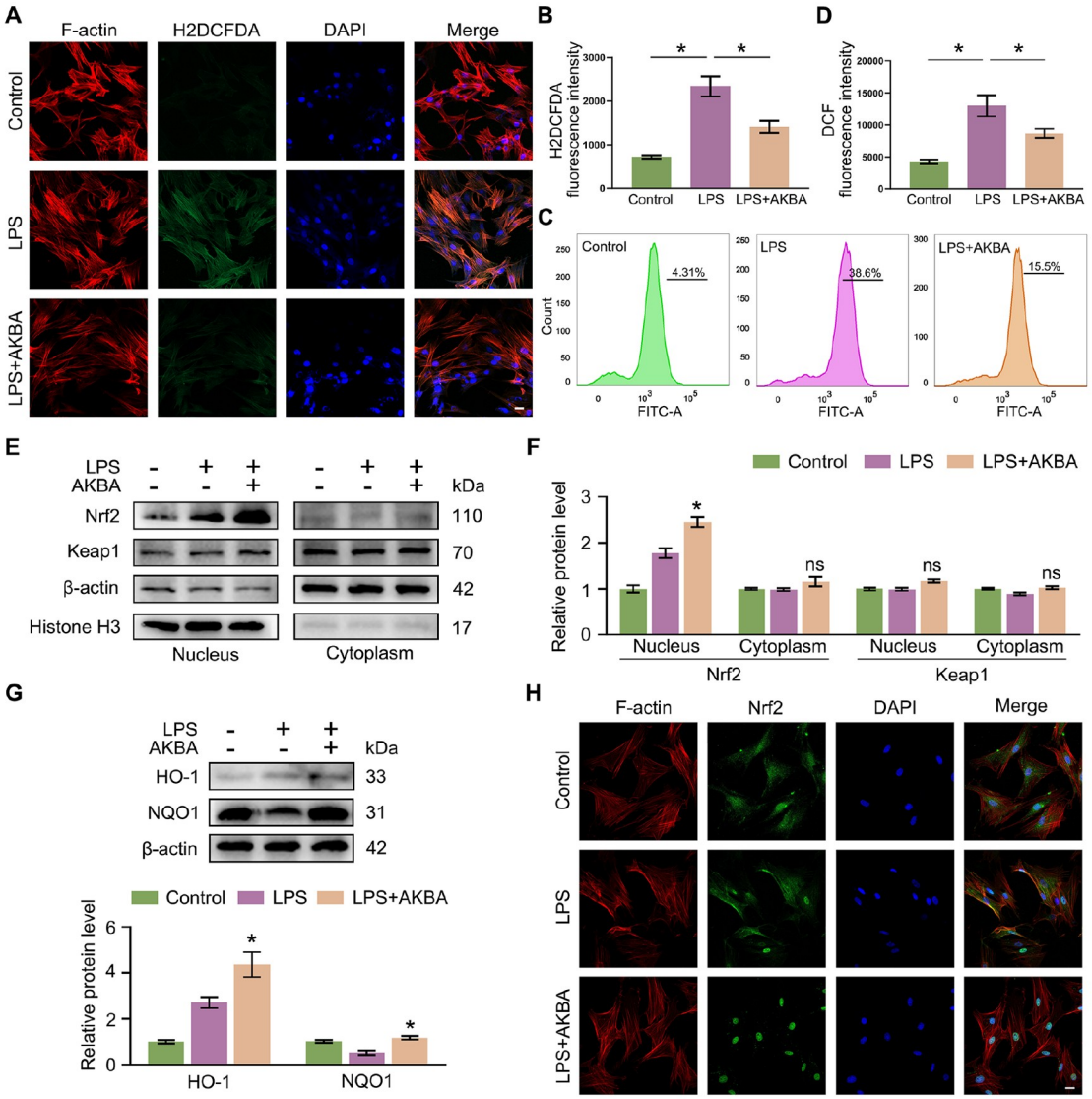

Figure 3. AKBA reduces ROS levels and increases the nuclear translocation of Nrf2 in FLSs (A,B) Immunofluorescence staining and quantitative analysis of ROS in FLSs; scale bar: 20 μm. (C,D) Flow cytometry and quantitative analysis of ROS in FLSs. (E) Representative western blots showing the nuclear and cytoplasmic expressions of Nrf2 and Keap1 in FLSs after LPS treatment and treatment with or without AKBA. (F) Quantification of the western blot data for Nrf2 and Keap1. (G) Representative western blots showing the expressions of HO-1 and NQO1 in FLSs after LPS treatment and treatment with or without AKBA. (H) Immunofluorescence staining for Nrf2 in FLSs; scale bar: 20 μm. Data are expressed as the mean±SD, n=3. *P<0.05 vs the LPS group.

ML385 suppresses the antioxidant effects of AKBA and inhibits the nuclear translocation of Nrf2 in FLSs

ML385 is a unique Nrf2 inhibitor that interacts directly with the Nrf2 protein by binding to the Neh1 binding region, consequently impeding the binding of the Nrf2-MAFG complex to the ARE sequence of the promoter and diminishing transcriptional activity [35]. Consequently, an investigation was conducted to assess the impact of ML385 on nuclear and cytoplasmic protein expression in FLSs treated with LPS and AKBA, with the aim of elucidating the potential involvement of the Nrf2 signaling pathway in the antioxidant effects of AKBA on FLSs under conditions of oxidative stress. According to the ROS levels determined by immunofluorescence staining and flow cytometry, ML385 treatment significantly increased ROS levels in AKBA-treated FLSs (Figure 4A–D). Furthermore, a notable decrease in Nrf2 expression in the nucleus was observed following stimulation with ML385, but no significant changes were detected in the cytoplasm (Figure 4E). Consistent with our expectations, changes in the expressions of proteins downstream

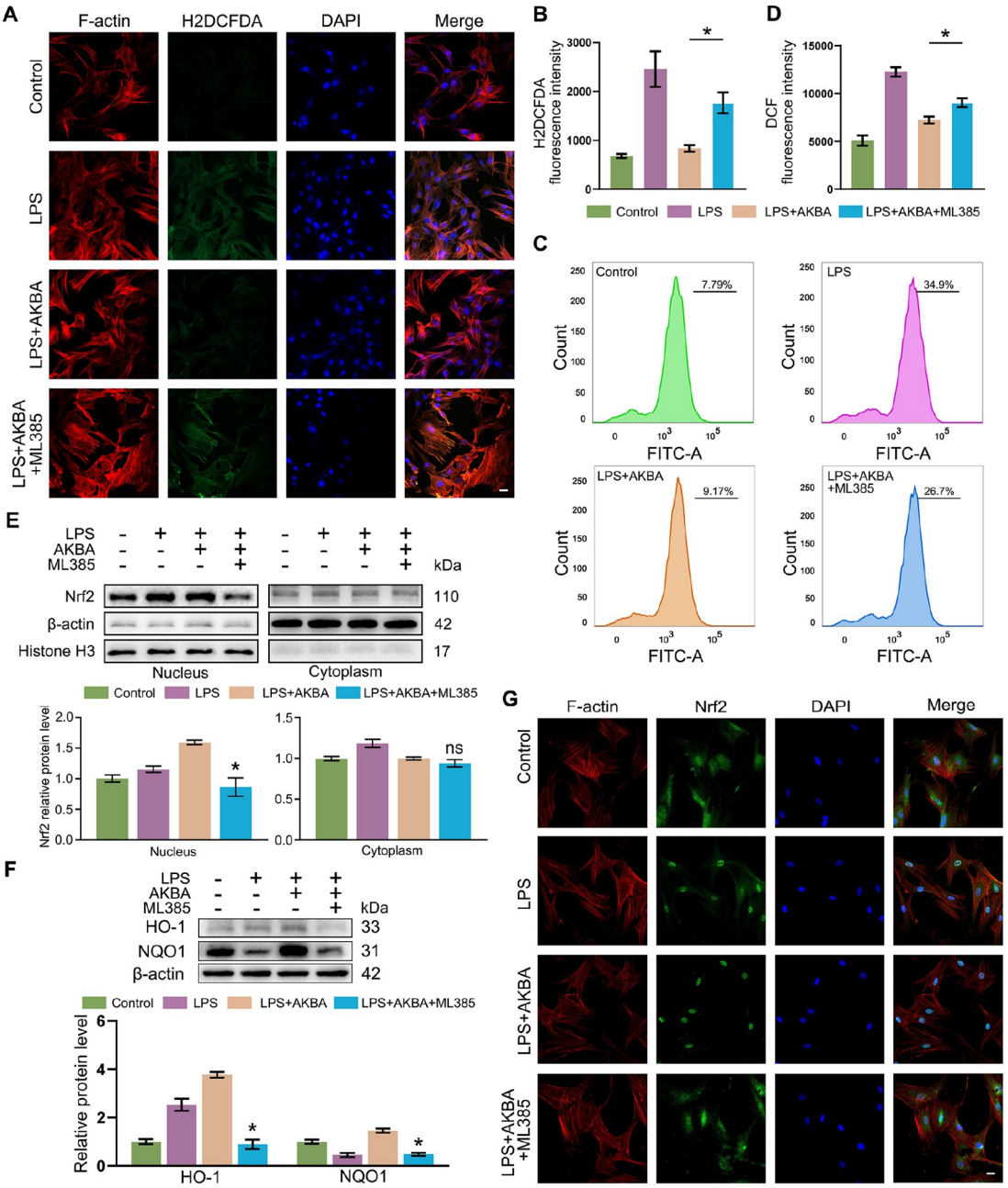

Figure 4. ML385 suppresses the antioxidant effects of AKBA and inhibits AKBA-mediated anti-inflammation and anti-MMP effects in FLSs (A,B) Immunofluorescence staining and quantitative analysis of ROS in FLSs; scale bar: 20 μm. (C,D) Flow cytometry and quantitative analysis of ROS in FLSs. (E) Representative western blots showing the nuclear and cytoplasmic expressions of Nrf2 in FLSs after LPS treatment or treatment with or without AKBA/ML385. (F) Representative western blots showing the expressions of HO-1 and NQO1 in FLSs after LPS treatment and treatment with or without AKBA/ML385. (G) Immunofluorescence staining for Nrf2 in FLSs; scale bar: 20 μm. Data are expressed as the mean±SD, n=3. *P<0.05 vs the LPS+AKBA group.

of Nrf2, namely, HO-1 and NQO1, were detected in the LPS+AKBA+ML385 group (Figure 4F). As shown in Figure 4G, the density of Nrf2 in the nucleus also exhibited a significant decrease after ML385 treatment, suggesting that the downregulation of the Nrf2 signaling pathway induced by ML385 inhibits the effects of AKBA.

ML385 reverses AKBA-mediated anti-inflammation and anti-MMP effects on FLSs

To further investigate the potential involvement of the Nrf2 signaling pathway in the effects of AKBA on FLS properties, migration and invasion assays were performed on AKBA-treated FLSs using the transwell chamber and cell scratch assay. The results indicated that ML385 notably attenuated both the migratory and invasive abilities of FLSs compared to those in the LPS+AKBA group (Figure 5A,B). Additionally, to validate the inhibitory effects of AKBA on the secretion of inflammatory cytokines and MMPs in FLSs through the Nrf2 signaling pathway, we analyzed changes in the expressions of inflammatory cytokines and MMPs in FLSs following treatment with LPS and AKBA in combination with ML385 treatment. Western blot analysis revealed that ML385 treatment increased the expressions of IL-1β, IL-6, TNF-α, iNOS, COX-2, MMP-1, MMP-3, and MMP-13 (Figure 5C,D). These results indicate that AKBA mitigates inflammation and MMP activity in FLSs by enhancing the Nrf2 signaling pathway.

AKBA alleviates pain, synovial inflammation, and fibrosis *in vivo*

In this study, an OA model was developed in rats through the transection of the medial collateral ligament, resection of the meniscus, and transection of the anterior cruciate ligament; this model is known as the ACLT+DMM model. The experimental protocol for the animal study is depicted in Figure 6A. At the beginning of the study, rats in the Sham group underwent surgical intervention involving the opening and closure of the joint cavity, while those in the OA group and OA+AKBA group underwent ACLT+DMM surgery. Following a two-week modeling period, the rats were intraperitoneally administered either 0.5 mL/kg saline or 8 mg/kg AKBA solution on alternate days for 4 weeks. After 8 weeks, all the experimental animals were euthanized, and samples were collected for subsequent analyses.

The body weights of the rats in the Sham, OA, and OA+AKBA groups remained stable prior to surgery, indicating a normal baseline (Figure 6B). Moreover, there were no significant differences in body weight among the groups, suggesting that AKBA administration did not have a significant impact on the growth or development of the rats. We evaluated alterations in nociceptive responses to mechanical stimuli after surgery through the assessment of the paw withdrawal mechanical threshold (PWMT) at biweekly intervals (Figure 6C). Both the OA group and the OA+AKBA group demonstrated decreased PWMTs in comparison to those of the Sham group, indicating the development of hyperalgesia in the OA-affected subjects. Nevertheless, rats in the OA+AKBA group exhibited elevated PWMTs in comparison to those in the OA group, indicating the efficacy of AKBA in mitigating enduring mechanical allodynia. Assessment of the maximal coronal diameter of the affected knee joint via Vernier calipers at biweekly intervals revealed a decrease in joint swelling in the AKBA-treated cohort as OA progressed (Figure 6D).

Synovial tissue was evaluated through pathological examination to analyze the influence of AKBA on synovial fibrosis in OA patients. H&E staining indicated a marked increase in the thickness of the synovial lining layer in the OA group, accompanied by the infiltration of inflammatory cells and small blood vessels. These alterations were significantly mitigated in the osteoarthritis group treated with AKBA (Figure 6E). Sirius Red staining revealed comparable findings, indicating a notable decrease in the synovitis score (Table 2) in the ACLT+DMM OA model following AKBA intervention (Figure 6F).

Immunohistochemical analysis of iNOS, MMP-13, Nrf2, and HO-1 (Figure 6G,H) further supported these results, showing a reduction in iNOS- and MMP-13-positive cells in the synovium after AKBA treatment, as well as a significant increase in Nrf2-positive areas in the OA+AKBA group compared to those in the OA and Sham groups. AKBA also increased the proportion of HO-1-positive cells following modeling, consistent with the *in vitro* findings, suggesting that AKBA may modulate synovial inflammation, extracellular matrix production, and synovial fibrosis via the Nrf2/HO-1 signaling pathway.

AKBA ameliorates chondrocyte extracellular matrix (ECM) degradation and ACLT+DMM-induced joint deterioration

Histological analysis and immunohistochemical staining were utilized to explore the efficacy of AKBA in preventing the degeneration of osteoarthritic joints. Safranin O-fast green and toluidine blue staining methods were used for histological analysis. The findings indicated that compared with those in the OA-only group, the proteoglycan loss in the cohort treated with both OA and AKBA decreased (Figure 7A). Additionally, the OA group exhibited concomitant cartilage layer thinning, chondrocyte depletion, and subchondral bone layer exposure. Subsequent to AKBA intervention, there was a partial reversal of these phenomena, as evidenced by the OARSI scores in each group (Figure 7B). Immunohistochemical analysis was performed to assess the levels of collagen type II (Col II) and MMP-13 expression in the articular cartilage of rats with OA. The results indicated a marked decrease in Col II expression and an increase in MMP-13 expression in chondrocytes within the OA group compared to those in the Sham group (Figure 7C,D). However, these effects were significantly attenuated by AKBA treatment.

In summary, the administration of AKBA has shown promise for attenuating extracellular matrix degradation in chondrocytes and reducing cartilage degeneration caused by ACLT+DMM.

Discussion

OA is a multifaceted joint pathology impacting a variety of anatomical structures, including muscles, subchondral bone, cartilage, ligaments, and synovial tissue [1,3–5,7,14,18]. The progression of fibrosis in the synovium during OA is subject to variation among individual patients and specific joint locations. This fibrogenesis process involves synovial hypertrophy and the formation of fibrotic masses, which contribute to the enduring joint pain and stiffness characteristics of OA [36–38]. FLSs, specialized mesenchymal cells, are integral to the lubrication of cartilage through the production of synovial fluid containing lubricin and hyaluronic acid [39,40]. In OA, activated FLSs release pro-inflammatory cytokines, chemokines, and proteolytic enzymes such as MMPs [41–44], which play a role in sustaining inflamma-

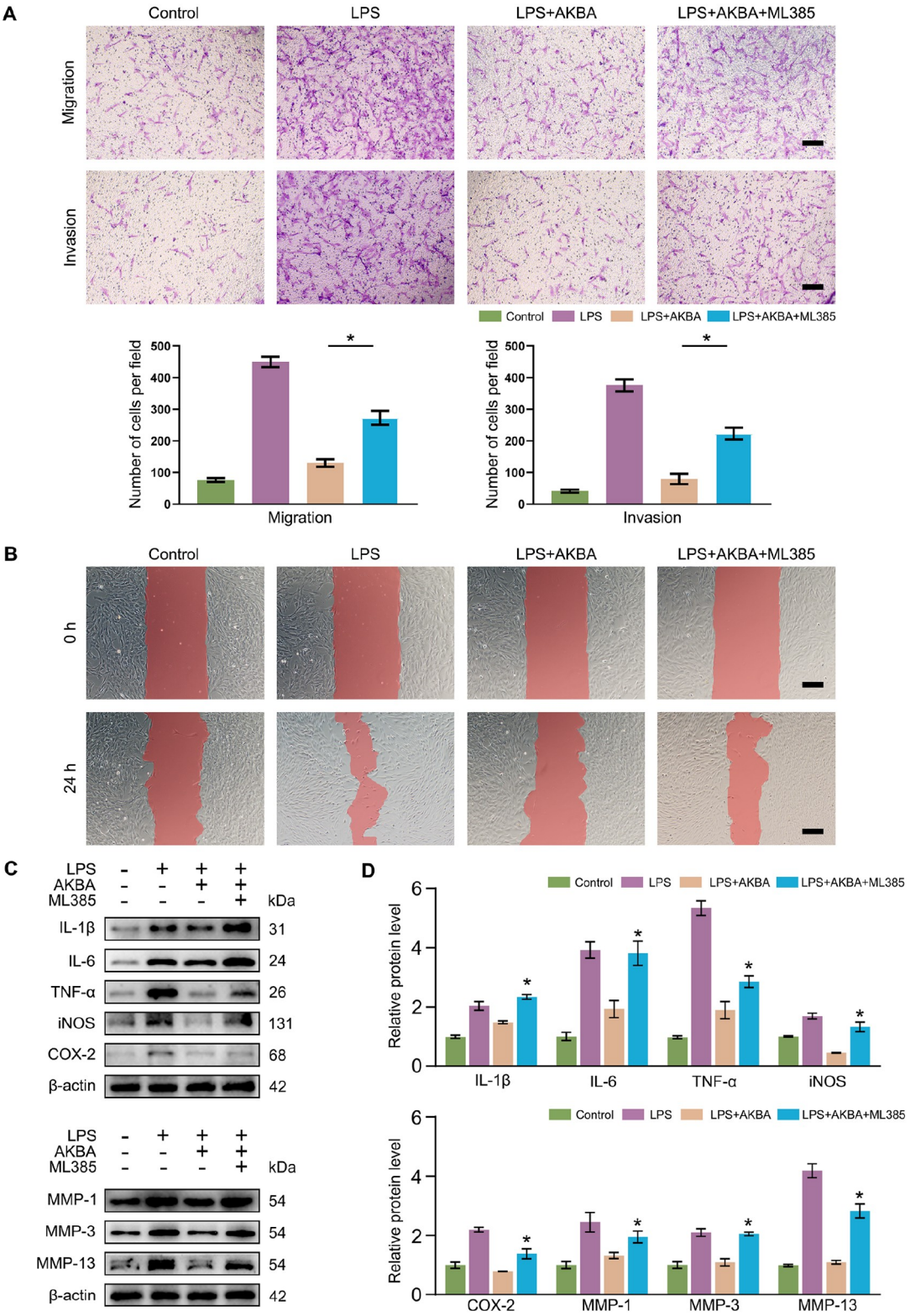

Figure 5. ML385 reverses the anti-inflammation and anti-MMP effects of AKBA on FLSs (A) Transwell migration and invasion assays and quantitative analysis of FLSs; scale bar: 200 μm. (B) Wound healing detected by a cell scratch assay; scale bar: 200 μm. (C,D) Representative western blots of inflammatory cytokines and MMPs protein expressions and quantitative analysis in FLSs after LPS treatment and treatment with or without AKBA/ML385. Data are expressed as the mean±SD, n=3. *P<0.05 vs the LPS+AKBA group.

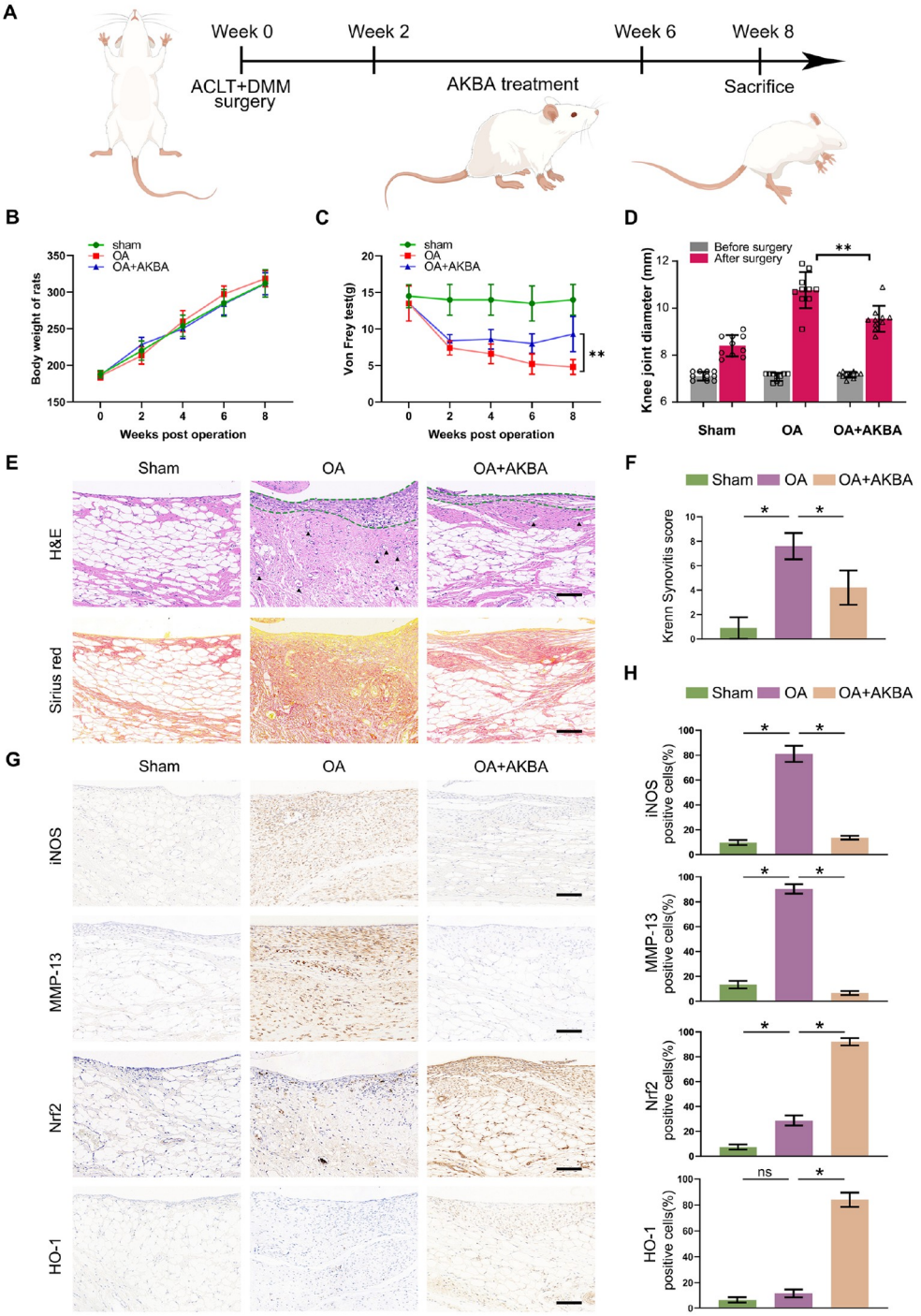

Figure 6. AKBA ameliorates pain, synovial inflammation and fibrosis *in vivo* (A) The experimental design for the animal study; Figure Draw ID: WOSPA7585e. (B) Changes in the body weight of the rats every 2 weeks after surgery. (C) Changes in pain sensitivity measured by the Von Frey test every 2 weeks after surgery. (D) Knee joint diameter of the right hind limbs of the rats before surgery and 6 weeks after surgery. (E) H&E and Sirius red staining of the synovium in different groups 6 weeks after surgery; scale bar: 100 μm. (F) Krenn synovitis scores of the synovium in different groups. (G) Immunohistochemical staining for iNOS, MMP-13, Nrf2, and HO-1 in the right hind joint synovium of rats; scale bar: 100 μm. (H) Percentages of iNOS-, MMP-13-, Nrf2-, and HO-1-positive cells. Data are expressed as the mean±SD, n=3. *P<0.05 vs. the OA group.

tion and degrading the cartilage matrix [45]. Hence, the targeted modulation of aberrantly activated FLSs represents a promising therapeutic strategy for OA. Our study demonstrated that AKBA, a pentacyclic triterpene compound, effectively mitigates inflammation, MMPs, and ROS in FLSs and joints via the Nrf2 pathway, thereby promoting the joint cartilage microenvironment. Furthermore, utilizing network pharmacology, we explored the potential role of AKBA in OA through the regulation of ROS production.

Table 2. Krenn synovitis score

	Score
Enlargement of the synovial lining cell layer	
The lining cells form one layer	0 points
The lining cells form 2–3 layers	1 point
The lining cells form 4–5 layers, few multinucleated cells might occur	2 points
The lining cells form more than 5 layers, the lining might be ulcerated and multinucleated cells might occur	3 points
Density of the resident cells	
The synovial stroma shows normal cellularity	0 points
The cellularity is slightly increased	1 point
The cellularity is moderately increased, multinucleated cells might occur	2 points
The cellularity is greatly increased, multinucleated giant cells, pannus formation and rheumatoid granulomas might occur	3 points
Inflammatory infiltrate	
No inflammatory infiltrate	0 points
Few mostly perivascular situated lymphocytes or plasma cells	1 point
Numerous lymphocytes or plasma cells, sometimes forming follicle-like aggregates	2 points
Dense band-like inflammatory infiltrate or numerous large follicle-like aggregates	3 points

In the context of OA progression, inflammation plays a significant role at the cellular level, primarily through the release of inflammatory cytokines by FLSs during OA development. These cytokines, including IL-1β, IL-6, TNF-α, iNOS, and COX-2, have been identified as key mediators in the pathogenesis of OA [46–49]. These results underscore the importance of inflammation in OA progression. Our study revealed that AKBA effectively inhibited LPS-induced inflammation in FLSs, as indicated by a notable decrease in the levels of proinflammatory cytokines, such as IL-1β, IL-6, TNF-α, iNOS, and COX-2. ROS-induced oxidative stress has been shown to negatively impact mitochondrial function in OA cells, leading to an increase in the production of inflammatory factors and MMPs in FLSs [11,34]. In addition to exogenous stimuli, FLSs are capable of initiating ROS production through the end respiratory burst response [50]. This detrimental cycle of inflammation and oxidative stress perpetuates the release of additional inflammatory mediators and ROS, ultimately worsening cartilage damage.

AKBA, a pharmacologically active pentacyclic triterpene compound found in *Boswellia serrata* extract, has been previously shown to alleviate inflammatory responses in various tissues, including those affected by diabetes, bronchial conditions, and nervous system disorders [51–53]. Previous research has shown that AKBA exerts its protective effects by scavenging ROS to prevent oxidative damage in rat macrophages and lens epithelial cells [28,54]. Given the limited oral bioavailability of AKBA, intraperitoneal injection was utilized in this study, allowing absorption through the mesentery. Our findings suggest that AKBA effectively mitigates synovial inflammation by suppressing the overproduction of ROS in FLSs. Our *in vivo* experiments confirmed the significant inhibitory effects of AKBA on inflammatory cell infiltration and fibrosis in the synovium. Both our *in vitro* and *in vivo* findings illustrated the potent anti-inflammatory effects of AKBA on OA-FLSs, including the suppression of MMPs secretion. Despite the potential efficacy of these therapeutic approaches, their application in the treatment of OA remains limited in the current literature. This study provides novel evidence indicating that AKBA effectively mitigates the disruption caused by LPS and anterior cruciate ligament transection combined with destabilization of medial meniscus-induced disturbances within the inflammatory microenvironment of the joint.

Nrf2 is a transcription factor located within the cell that contains antioxidant response elements (AREs) in the nucleus and modulates the expressions of genes responsible for maintaining redox balance, detoxification enzymes, and stress response proteins [55]. Our analysis revealed a strong correlation between AKBA treatment and activation of the Nrf2 pathway. The Nrf2 pathway is widely acknowledged for its involvement in anti-inflammatory and antioxidative mechanisms. The activation of Nrf2 leads to the upregulation of HO-1 expression, resulting in a reduction in inflammation and ECM degradation. Previous research has shown that Nrf2 deficiency is associated with increased NADPH oxidase 2 activity, while excessive downregulation of Nrf2 activation following Keap1 upregulation enhances NADPH oxidase 4 activity. This suggests that the interplay between Nrf2 and NADPH oxidase may play a crucial role in modulating the levels of ROS [56,57]. In the present study, the use of ML385 to suppress the expression of the Nrf2 gene demonstrated that AKBA plays a role in regulating ROS activation by modulating Nrf2, thereby affecting the inflammatory microenvironment in the synovium.

This study provides novel insights into the regulatory influence of AKBA on Nrf2 within the OA synovium, emphasizing the potent capacity of AKBA to mitigate synovial fibrosis, inflammatory cell infiltration, and cartilage degeneration during the progression of OA and associated pain. Furthermore, this research illustrates the significant role of Nrf2-dependent activation of phase II genes, including HO-1 and NQO1, in regulating the inflammatory response. Specifically, treatment with AKBA in combination with LPS led to an increase in the expression levels of HO-1 and NQO1 (Figure 8). However, numerous unresolved questions necessitate further investigation. For instance, the most effective molecular target and method of administration for modulating Nrf2 activity have not yet been determined, and the intricate interplay between Nrf2 and its upstream regulators remains largely unexplored. Additionally, it is recommended that the intraperitoneal administration and controlled release of AKBA be integrated with strategies for cartilage regeneration to enhance the efficacy of the drug and improve treatment outcomes for this disease.

In conclusion, the results of this study suggest that AKBA mitigates the progression of osteoarthritis and associated pain by virtue of its robust anti-inflammatory effects and its ability to inhibit MMPs and ROS, a mechanism that is facilitated through the Nrf2/HO-1 signaling pathway. Furthermore, AKBA has been shown to exhibit protective effects on the synovium and exert anti-inflammatory effects. Our findings provide support for the use of AKBA as a therapeutic intervention for OA and offer insights into the mechanisms underlying its positive effects on synovitis associated with this condition. This study lays the groundwork for the potential clinical use of AKBA in the treatment of OA, particularly in terms of managing disease progression and alleviating pain in affected individuals.

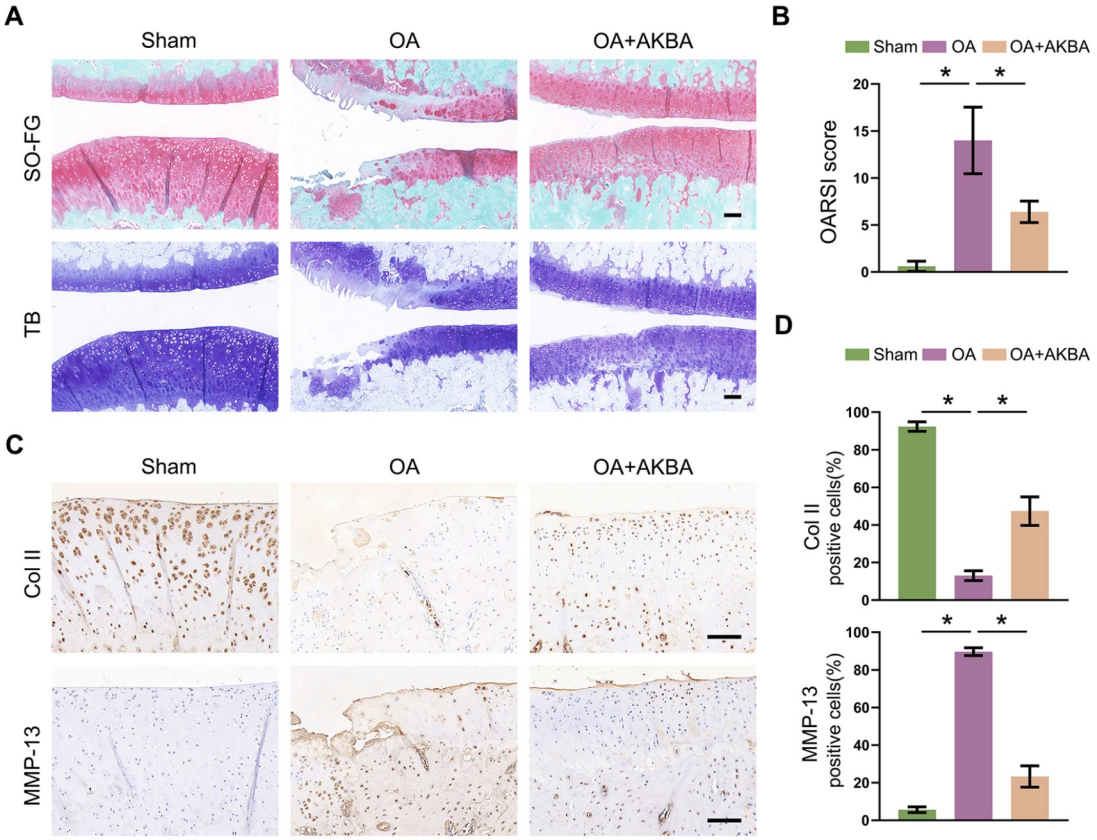

Figure 7. AKBA ameliorates ECM degradation in chondrocytes and ACLT+DMM-induced joint deterioration (A) Representative images of SO-FG and TB staining of knee joint sections from Sham-, OA-, and AKBA-treated OA rats; scale bar: 200 μm. (B) OARSI scores of the different groups. (C) Representative immunohistochemical staining of Col II and MMP-13; scale bar: 200 μm. (D) Percentage of positive cells for Col II and MMP-13. Data are expressed as the mean±SD, n=3. *P<0.05 vs the OA group.

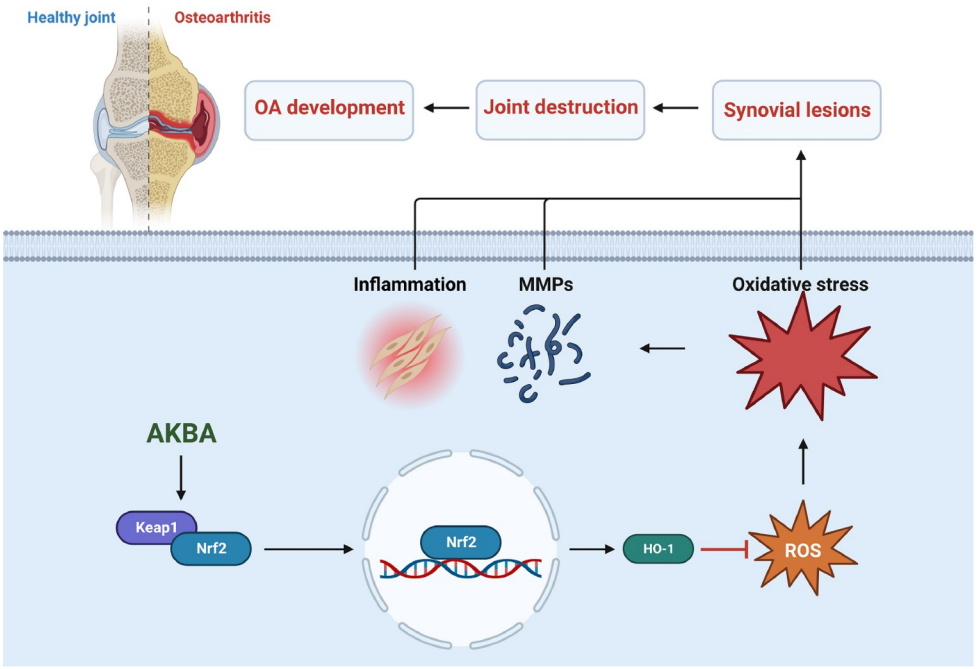

Figure 8. Schematic illustration of the Nrf2/HO-1 signaling activator AKBA-mediated antioxidative protection against OA

Acknowledgement

The authors are grateful to Dr Huaqiang Tao and Kai Chen of the Institute of Orthopedics, Soochow University for their technical support.

Funding

This work was supported by the grants from the National Natural Science Foundation of China (Nos. 82072425, 81873991, and 81672238), the Program of Jiangsu Science and Technology Department (Nos. BK20211083 and BE2022737), the Program of Suzhou Health Commission (Nos. GSWS2020078 and SZXK202111), the Program of Suzhou Science and Technology Department (No. SKY2023062), and the Jiangsu Graduate Student Cultivation Innovative Engineering Graduate Research and Practice Innovation Program (No. SJCX23_0683).

Conflict of Interest

The authors declare that they have no conflict of interest.

References

1. Katz JN, Arant KR, Loeser RF. Diagnosis and treatment of hip and knee osteoarthritis. *JAMA* 2021, 325: 568
2. Abdel-Aziz MA, Ahmed HMS, El-Nekeety AA, Abdel-Wahhab MA. Osteoarthritis complications and the recent therapeutic approaches. *Inflammopharmacology* 2021, 29: 1653–1667
3. Tong L, Yu H, Huang X, Shen J, Xiao G, Chen L, Wang H, *et al.* Current understanding of osteoarthritis pathogenesis and relevant new approaches. *Bone Res* 2022, 10: 60
4. Bernabei I, So A, Busso N, Nasi S. Cartilage calcification in osteoarthritis: mechanisms and clinical relevance. *Nat Rev Rheumatol* 2023, 19: 10–27
5. Hu W, Chen Y, Dou C, Dong S. Microenvironment in subchondral bone: predominant regulator for the treatment of osteoarthritis. *Ann Rheum Dis* 2021, 80: 413–422
6. Nedunchezhiyan U, Varughese I, Sun AR, Wu X, Crawford R, Prasadam I. Obesity, inflammation, and immune system in osteoarthritis. *Front Immunol* 2022, 13: 907750
7. Sanchez-lopez E, Coras R, Torres A, Lane NE, Guma M. Synovial inflammation in osteoarthritis progression. *Nat Rev Rheumatol* 2022, 18: 258–275
8. Maglaviceanu A, Wu B, Kapoor M. Fibroblast-like synoviocytes: role in synovial fibrosis associated with osteoarthritis. *Wound Repair Regen* 2021, 29: 642–649
9. Morris G, Gevezova M, Sarafian V, Maes M. Redox regulation of the immune response. *Cell Mol Immunol* 2022, 19: 1079–1101
10. McGarry T, Biniecka M, Veale DJ, Fearon U. Hypoxia, oxidative stress and inflammation. *Free Radic Biol Med* 2018, 125: 15–24
11. Marchev AS, Dimitrova PA, Burns AJ, Kostov RV, Dinkova-Kostova AT, Georgiev MI. Oxidative stress and chronic inflammation in osteoarthritis: can NRF2 counteract these partners in crime? *Ann NY Acad Sci* 2017, 1401: 114–135
12. Loboda A, Damulewicz M, Pyza E, Jozkowicz A, Dulak J. Role of Nrf2/HO-1 system in development, oxidative stress response and diseases: an evolutionarily conserved mechanism. *Cell Mol Life Sci* 2016, 73: 3221–3247
13. Li Q, Wen Y, Wang L, Chen B, Chen J, Wang H, Chen L. Hyperglycemia-induced accumulation of advanced glycosylation end products in fibroblast-like synoviocytes promotes knee osteoarthritis. *Exp Mol Med* 2021, 53: 1735–1747
14. Benito MJ, Veale DJ, FitzGerald O, van den Berg WB, Bresnihan B. Synovial tissue inflammation in early and late osteoarthritis. *Ann Rheum Dis* 2005, 64: 1263–1267
15. Chwastek J, Kędziora M, Borczyk M, Korostyński M, Starowicz K. Inflammation-driven secretion potential is upregulated in osteoarthritic fibroblast-like synoviocytes. *Int J Mol Sci* 2022, 23: 11817
16. De Roover A, Escribano-Núñez A, Monteagudo S, Lories R. Fundamentals of osteoarthritis: inflammatory mediators in osteoarthritis. *Osteoarthritis Cartilage* 2023, 31: 1303–1311
17. Yu DH, Yi JK, Yuh HS, Park Sj, Kim HJ, Bae KB, Ji YR, *et al.* Over-expression of extracellular superoxide dismutase in mouse synovial tissue attenuates the inflammatory arthritis. *Exp Mol Med* 2012, 44: 529–535
18. Wei Q, Zhu X, Wang L, Zhang W, Yang X, Wei W. Extracellular matrix in synovium development, homeostasis and arthritis disease. *Int Immunopharmacol* 2023, 121: 110453
19. Busa P, Lee SO, Huang N, *et al.* Carnosine alleviates knee osteoarthritis and promotes synoviocyte protection via activating the Nrf2/HO-1 signaling pathway: an *in-vivo* and *in-vitro* study. *Antioxidants (Basel)* 2022, 11: 1209
20. Kong R, Ji L, Pang Y, Zhao D, Gao J. Exosomes from osteoarthritic fibroblast-like synoviocytes promote cartilage ferroptosis and damage via delivering microRNA-19b-3p to target SLC7A11 in osteoarthritis. *Front Immunol* 2023, 14: 1181156
21. Ye X, Yin C, Huang X, Huang Y, Ding L, Jin M, Wang Z, *et al.* ROS/TGF-β signal mediated accumulation of SOX4 in OA-FLS promotes cell senescence. *Exp Gerontol* 2021, 156: 111616
22. Zhang L, Li X, Zhang H, Huang Z, Zhang N, Zhang L, Xing R, *et al.* Agnuside alleviates synovitis and fibrosis in knee osteoarthritis through the inhibition of HIF-1α and NLRP3 inflammasome. *Mediators Inflamm* 2021, 2021: 5534614
23. Li G, Liu S, Chen Y, Zhao J, Xu H, Weng J, Yu F, *et al.* An injectable liposome-anchored teriparatide incorporated gallic acid-grafted gelatin hydrogel for osteoarthritis treatment. *Nat Commun* 2023, 14: 3159
24. Shaban NS, Radi AM, Abdelgawad MA, Ghoneim MM, Al-Serwi RH, Hassan RM, Mohammed ET, *et al.* Targeting some key metalloproteinases by nano-naringenin and amphora coffeaeformis as a novel strategy for treatment of osteoarthritis in rats. *Pharmaceuticals (Basel)* 2023, 16: 260
25. De silva V, El-metwally A, Ernst E, Lewith G, Macfarlane GJ, Arthritis Research UK Working Group on Complementary and Alternative Medicines. Evidence for the efficacy of complementary and alternative medicines in the management of osteoarthritis: a systematic review. *Rheumatology (Oxford)* 2011, 50: 911–920
26. Ranzato E, Martinotti S, Volante A, Tava A, Masini MA, Burlando B. The major Boswellia serrata active 3-acetyl-11-keto-β-boswellic acid strengthens interleukin-1α upregulation of matrix metalloproteinase-9 via JNK MAP kinase activation. *Phytomedicine* 2017, 36: 176–182
27. Pan YN, Liang XX, Niu LY, Wang YN, Tong X, Hua HM, Zheng J. Comparative studies of pharmacokinetics and anticoagulatory effect in rats after oral administration of Frankincense and its processed products. *J Ethnopharmacol* 2015, 172: 118–123
28. Yuan C, Dong X, Xu S, Zhu Q, Xu X, Zhang J, Gong W, *et al.* AKBA alleviates experimental pancreatitis by inhibiting oxidative stress in Macrophages through the Nrf2/HO-1 pathway. *Int Immunopharmacol* 2023, 121: 110501
29. Li W, Liu J, Fu W, Zheng X, Ren L, Liu S, Wang J, *et al.* 3-O-acetyl-11-keto-β-boswellic acid exerts anti-tumor effects in glioblastoma by arresting cell cycle at G2/M phase. *J Exp Clin Cancer Res* 2018, 37: 132
30. Meyiah A, Shawkat MY, Ur Rehman N, Al-Harrasi A, Elkord E. Effect of Boswellic acids on T cell proliferation and activation. *Int Immunopharmacol* 2023, 122: 110668

31. Liu JJ, Toy WC, Liu S, Cheng A, Lim BK, Subramaniam T, Sum CF, *et al.* Acetyl-keto-β-boswellic acid induces lipolysis in mature adipocytes. *Biochem Biophys Res Commun* 2013, 431: 192–196
32. Pinamont WJ, Yoshioka NK, Young GM, Karuppagounder V, Carlson EI, Ahmad A, Elbarbary R, *et al.* Standardized histomorphometric evaluation of osteoarthritis in a surgical mouse model. *J Vis Exp* 2020, 159
33. Saha S, Rebouh NY. Anti-osteoarthritis mechanism of the Nrf2 signaling pathway. *Biomedicines* 2023, 11: 3176
34. Ansari MY, Ahmad N, Haqqi TM. Oxidative stress and inflammation in osteoarthritis pathogenesis: role of polyphenols. *Biomed Pharmacother* 2020, 129: 110452
35. Singh A, Venkannagari S, Oh KH, Zhang YQ, Rohde JM, Liu L, Nimmagadda S, *et al.* Small molecule inhibitor of NRF2 selectively intervenes therapeutic resistance in KEAP1-Deficient NSCLC tumors. *ACS Chem Biol* 2016, 11: 3214–3225
36. Scanzello CR, Goldring SR. The role of synovitis in osteoarthritis pathogenesis. *Bone* 2012, 51: 249–257
37. Remst DF, Blaney Davidson EN, van der Kraan PM. Unravelling osteoarthritis-related synovial fibrosis: a step closer to solving joint stiffness. *Rheumatology (Oxford)* 2015, 54: 1954–1963
38. Rim YA, Ju JH. The role of fibrosis in osteoarthritis progression. *Life (Basel)* 2021, 11: 3
39. Han D, Fang Y, Tan X, Jiang H, Gong X, Wang X, Hong W, *et al.* The emerging role of fibroblast-like synoviocytes-mediated synovitis in osteoarthritis: an update. *J Cell Mol Med* 2020, 24: 9518–9532
40. Nygaard G, Firestein GS. Restoring synovial homeostasis in rheumatoid arthritis by targeting fibroblast-like synoviocytes. *Nat Rev Rheumatol* 2020, 16: 316–333
41. Chenn Z, Lin CX, Song B, Li CC, Qiu JX, Li SX, Lin SP, *et al.* Spermidine activates RIP1 deubiquitination to inhibit TNF-α-induced NF-κB/p65 signaling pathway in osteoarthritis. *Cell Death Dis* 2020, 11: 503
42. Tolboom TC, Pieterman E, van der Laan WH, Toes RE, Huidekoper AL, Nelissen RG, Breedveld FC, *et al.* Invasive properties of fibroblast-like synoviocytes: correlation with growth characteristics and expression of MMP-1, MMP-3, and MMP-10. *Ann Rheum Dis* 2002, 61: 975–980
43. Lin Z, Ma Y, Zhu X, Dai S, Sun W, Li W, Niu S, *et al.* Potential predictive and therapeutic applications of small extracellular vesicles-derived circPARD3B in osteoarthritis. *Front Pharmacol* 2022, 13: 968776
44. Huh JE, Seo BK, Park YC, Kim JI, Lee JD, Choi DY, Baek YH, *et al.* WIN-34B, a new herbal medicine, inhibits the inflammatory response by inactivating IκB-α phosphorylation and mitogen activated protein kinase pathways in fibroblast-like synoviocytes. *J Ethnopharmacol* 2012, 143: 779–786
45. Li N, Chen Z, Feng W, Gong Z, Lin C, Chen J, Chu C, *et al.* Triptolide improves chondrocyte proliferation and secretion via down-regulation of miR-221 in synovial cell exosomes. *Phytomedicine* 2022, 107: 154479
46. Sluzalska KD, Liebisch G, Lochnit G, Ishaque B, Hackstein H, Schmitz G, Rickert M, *et al.* Interleukin-1β affects the phospholipid biosynthesis of fibroblast-like synoviocytes from human osteoarthritic knee joints. *Osteoarthritis Cartilage* 2017, 25: 1890–1899
47. Rzeczycki P, Rasner C, Lammlin L, Junginger L, Goldman S, Bergman R, Redding S, Knights AJ, *et al.* Cannabinoid receptor type 2 is upregulated in synovium following joint injury and mediates anti-inflammatory effects in synovial fibroblasts and macrophages. *Osteoarthritis Cartilage* 2021, 29: 1720–1731
48. Eymard F, Pigenet A, Citadelle D, Flouzat-Lachaniette CH, Poignard A, Benell C, Berenbaum F, *et al.* Induction of an inflammatory and prodegradative phenotype in autologous fibroblast-like synoviocytes by the infrapatellar fat pad from patients with knee osteoarthritis. *Arthritis Rheumatol* 2014, 66: 2165–2174
49. Wang CT, Lin YT, Chiang BL, Lin YH, Hou SM. High molecular weight hyaluronic acid down-regulates the gene expression of osteoarthritis-associated cytokines and enzymes in fibroblast-like synoviocytes from patients with early osteoarthritis. *Osteoarthritis Cartilage* 2006, 14: 1237–1247
50. Han Y, Wang J, Jin M, Jia L, Yan C, Wang Y. Shentong zhuyu decoction inhibits inflammatory response, migration, and invasion and promotes apoptosis of rheumatoid arthritis fibroblast-like synoviocytes via the MAPK p38/PPARγ/CTGF pathway. *Biomed Res Int* 2021, 2021: 6187695
51. AlTamimi JZ, AlFaris NA, Alshammari GM, Alagal RI, Aljabryn DH, Yahya MA. The protective effect of 11-Keto-β-Boswellic acid against diabetic cardiomyopathy in rats entails activation of AMPK. *Nutrients* 2023, 15: 1660
52. AMMON H P. Boswellic Acids and Their Role in Chronic Inflammatory Diseases. *Adv Exp Med Biol*, 2016, 928: 291–327
53. Li W, Ren L, Zheng X, Liu J, Wang J, Ji T, Du G. 3-O-Acetyl-11-keto-boswellic acid ameliorated aberrant metabolic landscape and inhibited autophagy in glioblastoma. *Acta Pharm Sin B* 2020, 10: 301–312
54. Yang T, Lin X, Li H, Zhou X, Fan F, Yang J, Luo Y, *et al.* Acetyl-11-Keto-beta boswellic acid (AKBA) protects lens epithelial cells against H2O2-Induced oxidative injury and attenuates cataract progression by activating keap1/Nrf2/HO-1 signaling. *Front Pharmacol* 2022, 13: 927871
55. Yamamoto M, Kensler TW, Motohashi H. The KEAP1-NRF2 system: a thiol-based sensor-effector apparatus for maintaining redox homeostasis. *Physiol Rev* 2018, 98: 1169–1203
56. Sies H, Jones DP. Reactive oxygen species (ROS) as pleiotropic physiological signalling agents. *Nat Rev Mol Cell Biol* 2020, 21: 363–383
57. Sies H. Findings in redox biology: from H_2O_2 to oxidative stress. *J Biol Chem* 2020, 295: 13458–13473